Intramolecular hydrogen tunneling in 2-chloromalonaldehyde trapped in solid para -hydrogen

Alejandro Gutiérrez-Quintanilla, Michèle Chevalier, Rasa Platakyte, Justinas Ceponkus, Claudine Crépin

ARTICLE

Intramolecular Hydrogen tunneling in 2-Chloromalonaldehyde trapped in solid para-hydrogen

Received 00th January 20xx,
Accepted 00th January 20xx

DOI: 10.1039/x0xx00000x

Alejandro Gutiérrez-Quintanilla,[a,b †] Michèle Chevalier,[a] Rasa Platakyte,[a,c] Justinas Ceponkus[c] and Claudine Crépin*[a]

Internal dynamics of 2-chloromalonaldehyde (2-ClMA) molecule, possessing strong internal hydrogen bond (IHB) was examined by means of matrix isolation spectroscopy in a soft host: *para*-hydrogen (pH$_2$). 2-ClMA is a chlorinated derivative of malonaldehyde (MA), a model molecule in hydrogen transfer studies, better suited to low temperature experiments than its parent molecule. The infrared absorption spectra of 2-ClMA isolated in pH$_2$ exhibit temperature dependent structures which are explained as transitions occurring from split vibrational levels induced by hydrogen tunneling. The doublet components associated with higher and lower energy levels are changing reversibly with the increase/decrease of the matrix temperature. The ground state splitting is measured to 7.9±0.1 cm^{-1}. The presence of oH$_2$ impurities in pH$_2$ matrix close to the neighborhood of the 2-ClMA molecule is found to quench the H tunneling. The data provide a powerful insight into the dynamical picture of intramolecular hydrogen tunneling in a molecule embedded in a very weakly perturbing environment.

1. Introduction

In a molecule with an intramolecular H bond (IHB), the hydrogen atom is shared, at least partially, between the donor and the acceptor and H transfer can be observed. Malonaldehyde (MA) and 2-Chloromalonaldehyde (2-ClMA) are prototype molecules with an IHB enhanced by a conjugated π electron system (resonance assisted H bond: RAHB) in their chelated enol forms. This structure favors the H transfer (see Fig. 1) which has been extensively studied theoretically for MA[1,2,3,4] and slightly less for 2-ClMA.[5,6,7] Infrared spectroscopy can bring key information on dynamics of this important and fundamental process in nature.[8] The H transfer between the two oxygens of MA has already been observed in the gas phase by means of a tunneling splitting of vibrational levels,[9,10,11] but seems to be blocked when MA is embedded in rare gas matrices.[12,13,14] Only very few studies describe the structure of 2-ClMA. We have recently published the first spectroscopic observation of that molecule trapped in different matrices to look at the environment effect on the most stable form, the chelated enol one (CCC - Fig. 1b), and also on some open conformers obtained after UV photolysis.[15,16] The infrared spectrum of CCC in *para*-hydrogen (pH$_2$) matrices shows a structure in some bands which suggests an H tunneling. In order to validate this hypothesis, new experiments were required.

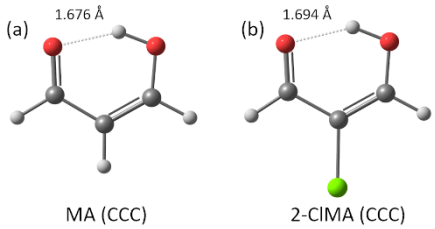

Fig. 1. MA and 2-ClMA in their chelated enol forms, named CCC, which are the most stable conformers. The marked -O···H- distances were obtained in DFT calculations at B3LYP/6-311++G(3df,3pd) level of theory; the corresponding O···O distances are 2.578 Å in 2-ClMA and 2.570 Å in MA at the same level of theory. The calculated structures indicate a slightly weaker IHB in 2-ClMA than in MA.

In the gas phase, the malonaldehyde tunneling splitting in the ground vibrational state was measured at $\Delta\nu_0$= 21.583 cm^{-1}.[17,18] pH$_2$ matrices, due to their quantum properties,[19,20,21,22] should preserve large amplitude motions such as H transfers in guest molecules and $\Delta\nu_0$ should not be significantly reduced in this specific matrix. Consequently, only the lowest level of MA is expected to be substantially populated in the temperature range reached in our experiments in solid pH$_2$ (2.8-5K). One more interesting candidate is the chlorinated derivative 2-ClMA because the presence of Cl in α-position in the pseudo cycle decreases the H bond strength, and thus increases the barrier height for the transfer. The O···O distance is slightly larger in 2-ClMA than in MA (see Fig. 1). $\Delta\nu_0$ should be smaller in 2-ClMA than in MA and the upper component of the ground state doublet could be weakly populated at 3K and

[a.] *Université Paris-Saclay, CNRS, Institut des Sciences Moléculaires d'Orsay, 91405, Orsay, France. * E-mail: claudine.crepin-gilbert@u-psud.fr*
[b.] *Instituto Superior de Tecnologías y Ciencias Aplicadas (InSTEC), Universidad de La Habana. Ave. Salvador Allende No. 1110, Quinta de los Molinos, La Habana 10400, Cuba.*
[c.] *Institute of Chemical Physics, Vilnius University, Sauletekio av. 9 bat. III, L-10222 Vilnius, Lithuania.*
† Present address: Aix-Marseille Université, Laboratoire PIIM, Team ASTRO, Service 252, Saint Jérôme, Ave. Escadrille Normandie Niemen, 13013 Marseille, France.
Electronic Supplementary Information (ESI) available: Part 1 -Table S1: details of the vibrational mode analysis; Part 2 - Table S2: details of the comparison with malonaldehyde. See DOI: 10.1039/x0xx00000x

significantly more at 5K. Numerous theoretical approaches were used to calculate $\Delta\nu_0$ in MA till recently.[2,23–27] In a previous work, Rios et al. predicted 22 cm^{-1} in MA and 12.2 cm^{-1} in 2-ClMA.[5] As the MA prediction is in very good agreement with the experiment,[18] a value close to 12 cm^{-1} for 2-ClMA is expected.

The aim of this paper is to reopen the discussion on how the H transfer modifies the vibrational pattern by analyzing new experimental data on 2-ClMA. The unique properties of the *para*-hydrogen matrix as a very low-disturbing environment are highlighted. At the same time, these results will allow to perform a quantification of the weak perturbation by probing a sensitive intrinsic property of the trapped molecule and comparing it to future gas phase experiments. We will give a simple interpretation of our observations; a complete theoretical interpretation is still lacking.

2. Methods

The experimental set-up was detailed in the Supporting Information of ref. 15. Briefly, *ortho/para*-hydrogen conversion process took place in a first cryostat (Air Products, Displex DE202). The hydrogen was condensed in a copper block located in this cryostat filled with Fe_2O_3 powder (Sigma-Aldrich 99 %) as catalyst and was left a few tens of minutes. Depending on the temperature (between 15 and 18 K) and on the conversion time, we obtained different degrees of purity for *para*-hydrogen. After conversion, the temperature of the cryostat was raised of some degrees and the gas was injected in front of a diamond window at about 3K in a second cryostat for the sample deposition (ICE: Innovative Cryogenic Engineering, RDK 415D, He Compressor: Sumitomo F-50). 2-ClMA (Acros, 95%) was used as supplied from the manufacturer. The reservoir containing 2-ClMA at room temperature was connected to the deposition tube, in which pH_2 was injected.

The *ortho*-hydrogen percentage (oH_2 %) was determined using the method proposed by Tam and Fajardo,[28,29] from the induced intensities of the lines $Q_1(0)+S_0(1)$ (4740 cm^{-1}) and $Q_1(0)$ (4153 cm^{-1}) of pH_2.

IR spectra were recorded between 700-5000 cm^{-1} with a FT-IR spectrometer (Nicolet Nexus 870) equipped with MCT detector. Most of the spectra were measured with a resolution of 0.5 cm^{-1}, with an accumulation of at least 500 scans. Wavenumbers of the peaks were obtained on all the samples to get average values and were also compared to the values obtained with some spectra at higher resolution (0.125 cm^{-1}). The accuracy varies from 0.1 to 0.5 cm^{-1} depending on the bands.

Computations were performed with the Gaussian 09 (revision A 02) program.[30] They were described in previous works.[15,16] Two methods were tested to get the mode frequencies of 2-ClMA. On one hand, we performed DFT calculations with M06-2X functional[31] and 6-311++G(3df,3pd) basis set, as detailed in the Supporting Information of ref. 15. On the other hand, we used the B3LYP functional[32,33] with the same basis set, as detailed in ref. 16. The use of two methods facilitates the analysis and discussion presented below.

3. Results

As described in our previous work,[15] the deposited 2-ClMA/pH_2 sample contains mainly the most stable conformer, the chelated CCC one, but two other open conformers are present in small amounts, about 10% for the first one (named TTC) and less than 1% for the other (named CTC). The CCC bands at 2.8K were discussed and assigned in this previous study, highlighting the presence of two clear doublets corresponding to vibrational modes around 1070 cm^{-1} and 915 cm^{-1}. The possibility of aggregate formation or presence of *fcc* sites in *hcp* pH_2 matrix cannot explain the presence of the observed doublets. A time evolution of the doublet bands was observed, pointing out the effect of oH_2 impurities in the sample. The detected very slow evolution was explained by the *ortho/para* conversion of these impurities, assuming that one component of each doublet contains the spectral contribution of 2-ClMA · oH_2 complexes.[34]

In this paper, we discuss the three parameters influencing the sample and consequently its spectrum: the initial *ortho*-hydrogen percentage, the time and the temperature, the two first parameters being coupled as previously explained.

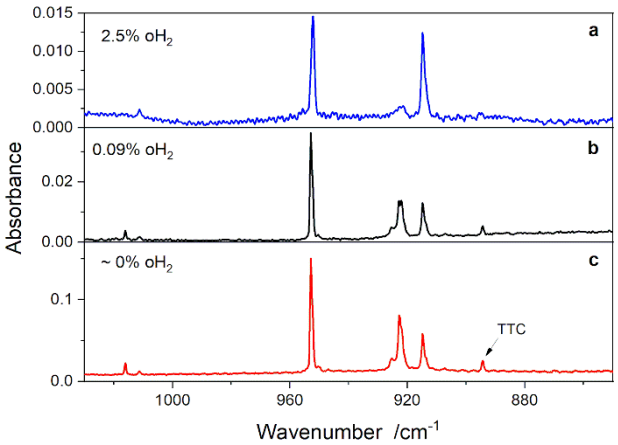

Fig. 2. Evolution of the spectra regarding the initial oH_2 % in the 1020-860 cm^{-1} region showing three modes of the CCC form: around 1011cm^{-1} (weak doublet), 952 cm^{-1} (single line) and 915 cm^{-1} (intense doublet). The additional band at 894.2 cm^{-1} belongs to an open conformer (TTC) as explained in ref.15.

Figure 2 shows the influence of the amount of oH_2 on the spectra of as-deposited samples at 2.8K. The displayed spectral range includes two intense modes: one around 915 cm^{-1} as a doublet and another around 952 cm^{-1} as a single line. A very weak third one around 1011 cm^{-1} is also a doublet, and the weak single line at 894.2 cm^{-1} belongs to another conformer (TTC). The most evident change occurs for the doublets. The peak at the higher frequency (HF) decreases for the benefit of that at the lower frequency (LF) when oH_2 % increases. It has nearly disappeared with 2.5 % of oH_2 in the sample. Table 1 gives the HF/LF ratio versus the oH_2 percentage for the intense doublet around 915 cm^{-1}. The trend is the same for the other intense doublet at 1070 cm^{-1}, the HF/LF ratio increases when the initial oH_2 % decreases, but the ratio values depend on the mode.

As oH_2 relaxes slowly to pH_2 by nuclear spin conversion (NSC), another way to vary oH_2 % in a sample is to wait after deposition.

We have left different samples in the dark for one to three days depending on the sample. The evolutions were the same in all the samples. The HF component increased, and the other decreased. The increase of the HF/LF ratio follows the measured decrease of oH$_2$ % by NSC, in agreement with the values reported in Table 1.

Table 1: Dependence of the intensity ratio HF/LF of the two components in the doublet around 915 cm^{-1} on the amount of *ortho*-hydrogen (oH$_2$ %).

oH$_2$ %	HF /LF
~0.0 (n.m.)	3.3
~0.0 (n.m.)	2.5
0.08	2.2
0.09	2.1
0.11	1.9
0.24	0.80
2.5	0.21

(n.m.): non measurable, HF: high frequency band, LF: low frequency band.

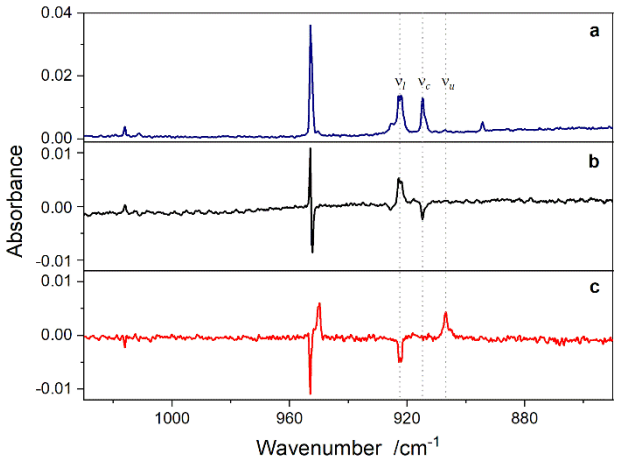

Fig. 3: Temporal evolution (irreversible) compared to the temperature effect (reversible) for three modes of the CCC form: around 1011cm^{-1} (very weak doublet, hardly visible), 952 cm^{-1} (single line) and 915 cm^{-1} (intense doublet). Spectrum of the as-deposited sample (a); difference spectrum between the spectrum of the sample after 3 days and that of the top panel [oH$_2$%=0.09] (b); difference spectrum between the spectrum of a sample heated at 5K and the spectrum of the same sample at 2.8K [oH$_2$%~0.0] (c). As an example, the ν_l, ν_c and ν_u components are labelled on the mode at ~915 cm^{-1}.

Figure 3 shows the time evolution in the same spectral range as that of Fig. 2 (panel b) and compares it to the evolution with temperature (panel c). The difference spectra bring new information. On the one hand, the mode at 952 cm^{-1} which looked like a single line in Fig. 2 is in fact a superposition of at least two peaks, the first one at 952.8 cm^{-1} increases and the second at 952.2 cm^{-1} decreases with time, i.e. with a decrease of oH$_2$ %. We observed such an evolution for all the CCC modes, not only those with well resolved doublets. These observations are in full agreement with our previous assumptions on the effect of oH$_2$.[34] We conclude that we can distinguish at least two components in the bands assigned to CCC modes in the spectra at 2.8K: one corresponds to the transition in 2-ClMA isolated in the pH$_2$ matrix - increasing with time - and the other, at least partially, to 2-ClMA solvated by oH$_2$ or to a complex between 2-ClMA and oH$_2$ - decreasing with time (HF and LF components of the previous discussion). The frequencies of these components, noted ν_l (*low* temperature) and ν_c (*complex*), are reported in Table 2 for all the observed modes. On the other hand, it is obvious in Fig. 3 that the changes in time (3b) are different from the changes induced by the temperature (3c). The ν_l components increase with a decrease of oH$_2$ % (positive peaks in Fig. 3b) and decrease with a temperature increase (negative peaks in Fig. 3c). Meanwhile, the ν_c components decrease with oH$_2$ % (negative peaks in Fig. 3b) but remain more or less stable in a temperature increase (no visible ν_c peaks in Fig. 3c). Importantly, new peaks are revealed at 5K for almost all the CCC modes. Their frequencies are reported as ν_u in Table 2.

When the temperature increases, the appearance of ν_u is correlated with a decrease of ν_l. It was not possible to record spectra at a temperature higher than 5K because of experimental constrains (hydrogen desorption). Going back to 2.8K, the effect was reversible: the ν_l components grew again and ν_u disappeared. This behaviour corresponds exactly to what was expected in the case of a tunneling splitting of the ground vibrational state of few wavenumbers: ν_l comes from the level of lowest energy (*lower* level) and ν_u from the level of highest energy (*upper* level), slightly populated at 5K, of the doublet.

Figure 4 shows the evolution of the spectrum with temperature. As expected, the observed effects are specific to the chelated CCC form, the only one involving an IHB. The TTC bands do not appear in the difference spectrum (see in particular the intense TTC band at 1152.8 cm^{-1} in Fig. 4). The ν_u components appear as upward peaks whereas the ν_l components appear as downward peaks in Fig. 4b. The change of intensity of ν_l or ν_u with the temperature, reflecting the population change in the ground state, allows to estimate the ground level splitting ($\Delta\nu_0$). The ν_l intensity decrease from 2.8K to 5K was measured as 7% on both lines at 922.7 and 1076.4 cm^{-1}, i.e. the HF components of the intense doublets. A Boltzmann analysis of the changes in intensity of the ν_l components leads to a rough value of $\Delta\nu_0$: $\Delta\nu_0 \sim 8$ cm^{-1}.

ARTICLE

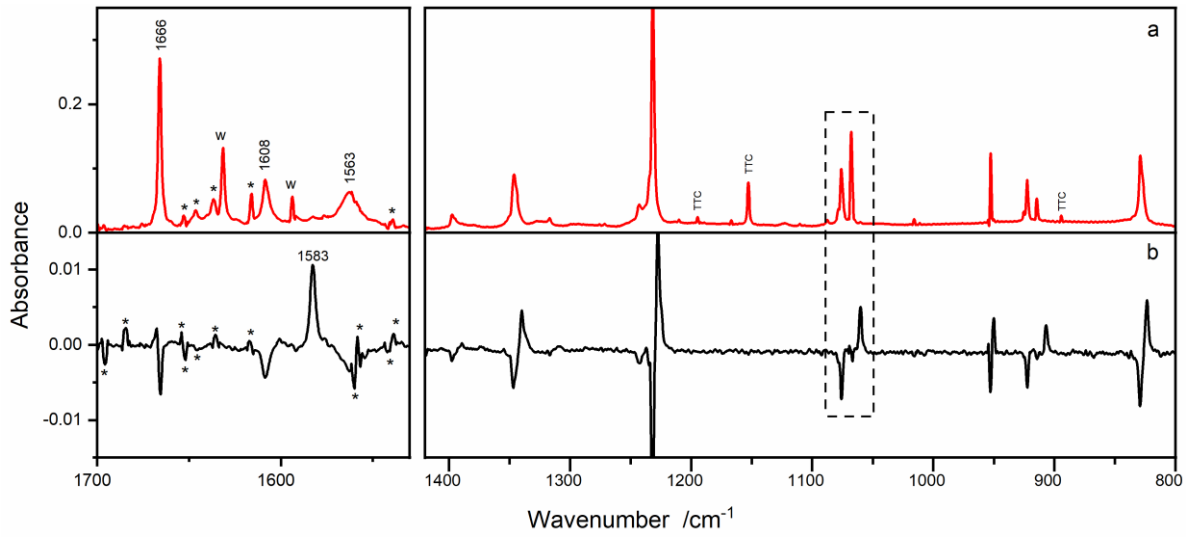

Fig. 4: Parts of the spectrum of 2-ClMA in a pH_2 matrix: sample at 2.8K (a), difference spectrum between sample heated at 5K and sample at 2.8K - 5K minus 2.8K - (b), the spectrum at 2.8K used in this difference spectrum is an average between the spectrum at 2.8K before annealing at 5K and the spectrum at 2.8K after annealing, in order to get rid of the changes in time. A zoom of the range included in the dotted rectangle is presented in Figure 6. Left panel: w: water bands, * bad compensation of atmospheric bands, marked numbers are wavenumbers of 2-ClMA vibrational bands included in the corresponding spectral range. Right panel: TTC denotes the bands belonging to that isomer.

Table 2. Experimental frequencies of the multiplet structure observed on various vibrational modes of 2-ClMA in a pH_2 matrix, theoretical characteristics of these modes and associated tunneling splitting ($\Delta\nu_1$).

N°	Experiment			Calculations			
	ν_l	ν_c	ν_u	Mode description	frequency (intensity)	$\nu_l - \nu_u$	$\Delta\nu_1$
20 (ip)	*2910*	*2910*	*2897*	νCH(alcohol)/νOH(iph)	3169.5 (113)	~13	~7
19 (ip)	2878	2876	2870.5	νCH(ketone)	3002 (50)	~7	~1
18 (ip)	1666	1665.8	1666.5	(νC=O / νC=C) (oph)	1700.7 (154)	-0.5	8.4
17 (ip)	*1608* 1563	*Not well defined*	1583	δOH/(νC=O/νC=C) (iph)	1613.2 (237)	*25* -20	28 [a]
16 (ip)	1398	1395	1390	(δCHs + δCH) (iph)	1421.6 (26)	8	0
15 (ip)	1347.5	1345	1340	δOH	1383.1 (103)	7.5	0.4
14 (ip)				(δCHs + δCH) (oph)	1371.4 (64)		
13 (ip)	*1235* 1232.2	1230.7	*1224.8* 1227.5	δOH/ δCH(alcohol)	1271.9 (200)	*10.2* 4.7	3.2 [b]
12 (ip)	1076.4	1068.2	1060.2	νC-C/δCCC/νC-Cl	1080.1 (81)	16.2	8.3
11 (oop)	*1016*	*1011*		(γCHs + γCH) (oph)	1034.6 (5)		
10 (oop)	952.8	952.2	950	(γCHs + γCH) (iph)	997.1 (41)	2.8	5.1
9 (ip)	922.7	914.8	907	Δ + δOH + νC-Cl	926.1 (35)	15.7	7.8
8 (oop)	829.5	827	823.5	γOH	909.1 (53)	6	1.9

Notes: ν_l, ν_c and ν_u: components assigned to transitions from the *lower* level (*l*) of the ground state doublet, from 2-ClMA complexes with oH_2 (*c*) and from the *upper* level (*u*) of the ground state doublet, respectively; frequencies in cm^{-1}. *Italics*: very weak bands for which effects are hardly detected or whose identification is not completely clear. Calculations performed on 2-^{35}ClMA at the B3LYP/6-311++G(3df,3pd) level of theory: mode frequencies (cm^{-1}) and intensities (km/mol) in parenthesis together with a simplified description of the modes (ν- stretching, δ-in plane bending, γ-out of plane bending, Δ -in plane ring deformation, (oph) out of phase, (iph) in phase). $\Delta\nu_1 = |\nu_l - \nu_u - \Delta\nu_0|$ (cm^{-1}) is the tunneling splitting for the corresponding mode, assuming $\Delta\nu_0$=7.9 cm^{-1} in the ground state. Mode numbering comes from the numbers in Tables S1 and S2 in ESI; ip: in-plane mode, oop: out-of-plane mode.

[a] obtained with (ν_l, ν_u)=(1563,1583) - see text. [b] value deduced from the main ν_l and ν_u components.

All the CCC bands exhibit temperature and oH_2 effects. However, they were hardly or even not detected in the weakest bands: only one value is reported for these bands in Table 2, as ν_l. Table 2 reports also the theoretical frequencies and IR intensities of the modes of 2-^{35}ClMA (B3LYP/6-311++G(3df,3pd) calculations)[16] together with a description of these modes. The intensity decrease correlated with a diminution in oH_2 % concerns (when observed) only one component for a given mode. We conclude that the presence of oH_2 in the neighborhood of 2-ClMA blocks the tunneling process, leading to only one line for each mode in 2-ClMA·oH_2 complexes. One can also notice that ν_c frequencies are very close to the vibrational frequencies measured in Ne (see Table 2, ref.15)

4. Discussion

The vibrational modes of 2-ClMA are theoretically well described considering 2-ClMA as a planar molecule with a C_s symmetry (see Table 2 and ref.15). Due to the tunneling, the vibrational levels are split into two sublevels labelled (*l*) for the lower and (*u*) for the upper. Considering one vibrational mode described in the C_s symmetry, there are three possible cases of transitions from the sublevels (l_0, u_0) of the ground state: either only the l_0-l_1 and u_0-u_1 transitions are observed (①), or only the l_0-u_1 and u_0-l_1 ones (②), or the four transitions - hybrid modes - (③) (see Fig.5, top panel).[35] In the last case, the absorption spectrum from l_0 gives directly the value of the tunneling splitting in the excited state ($\Delta\nu_1$). We observed that the LF peak (ν_c) of the intense doublets and especially of the doublet around 1070 cm^{-1} remained always present even with a very low oH_2 %, suggesting that the ν_c component hides another band. There is in fact an overlap between the component due to 2-ClMA·oH_2 complexes and the l_0-l_1 component of the vibrational transition. As a hybrid transition, the HF component corresponds obviously to the l_0-u_1 transition. A trace of this overlap is observable around 1070 cm^{-1}, where the l_0-l_1 and u_0-u_1 bands appear in the difference spectrum in which the component due to 2-ClMA·oH_2 is not present (see Fig. 6). In these doublets $\nu_l - \nu_u = \Delta\nu_0 + \Delta\nu_1$. The value $\Delta\nu_0$=7.9 ± 0.1 cm^{-1} is deduced from a careful analysis of the doublet around 1070 cm^{-1} in the spectra of different samples, in perfect agreement with the rough estimation previously mentioned. With such a $\Delta\nu_0$ value, u_0 is very weakly populated (<2%) at 2.8 K whereas its population reaches approximately 10% at 5K. It explains that the ν_u component was barely or even not visible at the lowest temperature. The vibrational effect on the tunneling is thus highlighted by the value of the splitting in the excited vibrational level $\Delta\nu_1$, deduced from $\nu_l - \nu_u$ for each mode: $\Delta\nu_1 = |\nu_l - \nu_u - \Delta\nu_0|$ (Table 2).

Fig. 5: Top panel: vibrational transitions and tunneling sublevels at play with the three cases described in the text ①, ②, and ③. Bottom panel: symmetries of the sublevels in the four symmetry cases of vibrational modes and the correlated allowed transitions from l_0 with the involved component of $\boldsymbol{\mu}$. The possible ①, ②, and/or ③ cases are reported in each mode symmetry. Red (black) arrows for transitions from the lower (upper) level of the ground state doublet.

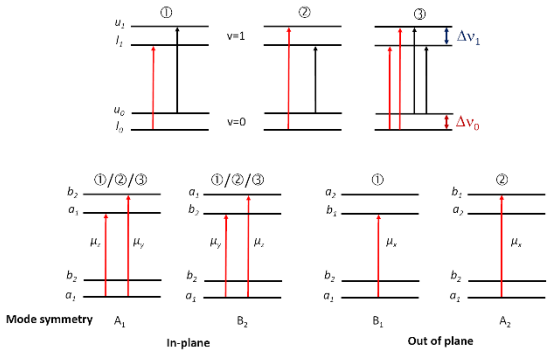

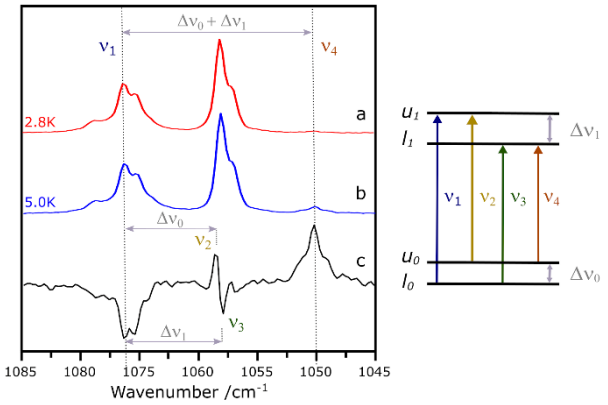

Fig. 6: Left panel: details of the spectra of 2-ClMA in a pH_2 matrix in the spectral range of the mode around 1070 cm^{-1}: sample at 2.8 K (a), sample at 5K (b), difference spectrum [(b)-(a)] (c). Right panel: scheme of the levels at play in the vibrational transition. Vibrational frequencies (ν_i, *i*=1-4)) are numbered from the highest value to the lowest one. They are marked in both panels, together with the tunneling splittings ($\Delta\nu_0$ and $\Delta\nu_1$). In this specific mode, the ν_l and ν_u components reported in Table 2 correspond to ν_1 and ν_4 respectively.

Taking into account the H tunneling, 2-ClMA belongs to the molecular symmetry group G_4 isomorphic to the C_{2v} point group.[35,36,37,38] Using the C_{2v} symmetry labels, l_0 belongs to symmetry a_1 and u_0 to symmetry b_2. Vibrational levels of in-plane modes give rise to doublets (l_1, u_1) of a_1 and b_2

symmetries and out-of-plane modes to a_2 and b_1 (l_1, u_1) doublets (see Fig. 5). Molecular axis are chosen in relation with the transient C_{2v} molecule with *z* axis close to the C-Cl axis and including the middle position of the transferring H, *y* axis perpendicular to *z* axis in the molecular plane, and *x* axis perpendicular to the molecular plane.[38] a_1-a_1, a_1-b_2 and a_1-b_1 transitions are allowed via the *z*, *y* and *x* components (μ_z, μ_y, and μ_x) of the transition dipole moment ($\boldsymbol{\mu}$), respectively. Consequently, only one vibrational transition is symmetry allowed from l_0 (or u_0) to one component of the doublet in out-of-plane modes (the a_1-b_1 component) whereas transitions to both components are symmetry allowed for in-plane modes. The intensity ratio between the two components depends on the orientation of the transition dipole moment in the molecular frame. Hybrid transitions correspond thus to vibrational transitions with non-vanishing μ_y and μ_z components of $\boldsymbol{\mu}$. We can consider the direction of $\boldsymbol{\mu}$ obtained in the visualization of the vibrational modes calculated in C_s symmetry to estimate μ_y/μ_z for the different in-plane modes observed in our spectra (see ESI, Table S1). In order to get insight in vibrational effects on the tunneling splitting deduced from the experiments, we also compared the frequencies of the vibrational modes of 2-ClMA in the equilibrium configuration (C_s) and in the transition state for H transfer (C_{2v}) at the same level of theory. The resulting analysis for all the vibrational modes is detailed in Part 1 of ESI.

Whilst only one transition from l_0 is observed in most of the modes, the calculated transition dipole moment of many in-plane modes has substantial μ_y and μ_z components, predicting hybrid modes. In fact, three hybrid modes are observed. The most obvious one corresponds to the intense doublet around 1070 cm^{-1}: HF/LF~1 was recorded in pure *p*H_2 samples, in agreement with $\mu_y/\mu_z \sim 1$ theoretically obtained for this transition (see ESI, Table S1). Similarly, $\mu_y/\mu_z \geq 2$ is observed from the calculations for the other doublet around 915 cm^{-1}, in agreement with the first row of Table 1. The third one is detected around 1230 cm^{-1}: the transition appears mainly with a ① behavior, but shoulders (blueshifted for ν_l and redshifted for ν_u) indicate a ③ behavior (cf Fig. 5). The three modes in the 1300-1400 cm^{-1} region are also predicted as hybrid modes. Experimentally, only two bands are detected at low temperature. The band at 1347.5 cm^{-1} could hide two vibrational modes, theoretically calculated at 1383 and 1371 cm^{-1}. As $\Delta\nu_1$ is measured close to zero, both ν_l components could overlap for each mode, explaining the apparent width of the bands.

A puzzling case concerns the intense mode theoretically predicted at 1613 cm^{-1}: it appears with two ν_l components at 1608 and 1563 cm^{-1} and only one ν_u component at 1583 cm^{-1}. Moreover, the corresponding value of ν_c remains uncertain because this component seems hidden by water bands in the vicinity. From theoretical considerations, this mode is predicted with a ① behavior (see ESI, Table S1), meaning that the (ν_l, ν_u) pair could be (1563 cm^{-1}, 1583 cm^{-1}). This assignment suggests $\Delta\nu_1$=28 cm^{-1}, *i.e.* a large enhancement of the tunneling splitting upon this vibrational excitation. A possible origin of the two bands observed in the spectrum at low temperature is a Fermi resonance,[15] an explanation in agreement with the spectrum obtained in Ne[15] where the mode at play cannot be assigned to a single band whereas no tunneling splitting was detected. In fact, a second very large ν_u band is not excluded (as detailed in ESI, Part 1). Consequently, the $\Delta\nu_1$ value for this mode remains uncertain. Besides, the similarities of frequencies in C_s and C_{2v} geometries (Table S1) and the comparison with MA (Table S2 in ESI) would suggest $\Delta\nu_1 \sim \Delta\nu_0$.

The comparison of the relative splitting of the vibrational modes ($\Delta\nu_1/\Delta\nu_0$) in MA and 2-ClMA is given in ESI, Table S2. The values are close except for the modes involving the OH bending around 1350 cm^{-1} and 1613 cm^{-1} in both molecules. In MA the former one enhances the tunneling while an enhancement is only possible for the latter one in 2-ClMA. The former mode possibly overlap with another mode in the 2-ClMA spectrum, but the conclusion of a very weak $\Delta\nu_1$ seems unquestionable, in contrast with the strong enhancement of the tunneling with this mode in MA, which was experimentally observed and theoretically predicted.[11,25] The correspondence between MA and 2-ClMA modes in this frequency range (and their symmetries) is not obvious.

5. Conclusions

In summary, we report clear evidence of H transfer along an IHB in a molecule embedded in a *p*H_2 matrix for the first time. The tunneling splitting of vibrational levels was very scarcely observed in cryogenic matrices.[15] In particular, the tunneling in MA was found to be quenched in rare gas matrices.[12,13,14] The present study confirms the property of the specific *p*H_2 matrix to preserve large amplitude motions. The tunneling splitting in the ground state (7.9 cm^{-1}) is close to the predicted one (12 cm^{-1})[5] for the isolated molecule. A slowing down of the H transfer or negligible effect with vibrational excitation was observed depending on the explored mode. The comparison with the vibrational effects in MA, especially on vibrational modes enhancing the tunneling is puzzling. Indeed, the theoretical works devoted to calculations of the tunneling splittings in the vibrational modes have been done in MA [24,25,27] but are lacking for 2-ClMA. Our results can be used for similar calculations and can help to improve the theoretical models. Another interesting result is the quenching of the tunneling with *o*H_2 in the neighborhood of 2-ClMA. This quenching was observed in Ne and the tunneling effect is found to be quenched or reduced in Ar.[15,39]

.

Conflicts of interest

There are no conflicts to declare.

Acknowledgements

The authors are grateful to Prof. M. Suhm and Dr. F. Gatti for helpful discussions. They acknowledge the use of the computing center MésoLUM of the LUMAT research federation (FR LUMAT 2764). This work was supported by the RTRA Triangle de la Physique (2013-0436T REACMAQ) and benefited from the French-Lithuanian PHC GILIBERT program (42125XF and S-LZ-19–1 from RCL) and the French-Cuban PHC Carlos J. Finlay program (41805NA).

References

1 F. Wu, *J. Phys. Chem. A*, 2016, **120**, 3849–3854.
2 M. Schröder, F. Gatti and H. D. Meyer, *J. Chem. Phys.*, 2011, **134**, 234307.
3 D. P. Tew, N. C. Handy and S. Carter, *J. Chem. Phys.*, 2006, **125**, 084313.
4 Y. Wang, B. J. Braams, J. M. Bowman, S. Carter and D. P. Tew, *J. Chem. Phys.*, 2008, **128**, 1–9.
5 M. A. Rios and J. Rodriguez, *J. Mol. Struct.*, 1991, **228**, 149–158.
6 J. N. Woodford, *J. Phys. Chem. A*, 2007, **111**, 8519–8530.
7 E. Nakhaei and A. Nowroozi, *Comput. Theor. Chem.*, 2016, **1096**, 27–32.
8 K. Giese, M. Petković, H. Naundorf and O. Kühn, *Phys. Rep.*, 2006, **430**, 211–276.
9 S. L. Baughcum, R. W. Duerst, W. F. Rowe, Z. Smith and E. B. Wilson, *J. Am. Chem. Soc.*, 1981, **103**, 6296–6303.
10 N. O. B. Lüttschwager, T. N. Wassermann, S. Coussan and M. A. Suhm, *Mol. Phys.*, 2013, **111**, 2211–2227.
11 N. O. B. Luttschwager, T. N. Wassermann, S. Coussan and M. A. Suhm, *Phys. Chem. Chem. Phys.*, 2010, **12**, 8201–8207.
12 T. N. Wassermann, D. Luckhaus, S. Coussan and M. A. Suhm, *Phys. Chem. Chem. Phys.*, 2006, **8**, 2344–2348.
13 D. W. Firth, P. F. Barbara and H. P. Trommsdorff, *Chem. Phys.*, 1989, **136**, 349–360.
14 T. Chiavassa, P. Verlaque, L. Pizzala, A. Allouche and P. Roubin, *J. Phys. Chem.*, 1993, **97**, 5917–5925.
15 A. Gutiérrez-Quintanilla, M. Chevalier, R. Platakyte, J. Ceponkus, G. A. Rojas-Lorenzo and C. Crépin, *Phys. Chem. Chem. Phys.*, 2018, **20**, 12888–12897.
16 A. Gutiérrez-Quintanilla, M. Chevalier, R. Platakyte, J. Ceponkus and C. Crépin, *J. Chem. Phys.*, 2019, **150**, 034305.
17 S. Baughcum, Z. Smith, E. Wilson and R. Duerst, *J. Am. Chem. Soc.*, 1984, **106**, 2260–2265.
18 T. Baba, T. Tanaka, I. Morino, K. M. T. Yamada and K. Tanaka, *J. Chem. Phys.*, 1999, **110**, 4131–4133.
19 M. Dusseault and M. Boninsegni, *Phys. Rev. B*, 2017, **95**, 104518.
20 T. Momose, H. Hoshina, M. Fushitani and H. Katsuki, *Vib. Spectrosc.*, 2004, **34**, 95–108.
21 I. F. Silvera, *Rev. Mod. Phys.*, 1980, **52**, 393–452.
22 R. R. Lozada-García, J. Ceponkus, M. Chevalier, W. Chin, J. M. Mestdagh and C. Crépin, *Angew. Chemie - Int. Ed.*, 2012, **51**, 6947–6950.
23 A. Viel, M. D. Coutinho-Neto and U. Manthe, *J. Chem. Phys.*, 2007, **126**, 24308.
24 T. Hammer, M. D. Coutinho-Neto, A. Viel and U. Manthe, *J. Chem. Phys.*, 2009, **131**, 224109.
25 T. Hammer and U. Manthe, *J. Chem. Phys.*, 2012, **136**, 054105.
26 F. Wu, Y. Ren and W. Bian, *J. Chem. Phys.*, 2016, **145**, 074309.
27 M. Schröder and H. D. Meyer, *J. Chem. Phys.*, 2014, **141**, 034116.
28 S. Tam and M. E. Fajardo, *Rev. Sci. Instrum.*, 1999, **70**, 1926–1932.
29 M. E. Fajardo and S. Tam, *J. Chem. Phys.*, 1998, **108**, 4237–4241.
30 M. J. Frisch, G. W. Trucks, H. B. Schlegel, G. E. Scuseria, M. A. Robb, J. R. Cheeseman, G. Scalmani, V. Barone, B. Mennucci, G. A. Petersson, H. Nakatsuji, M. Caricato, X. Li, H. P. Hratchian, A. F. Izmaylov, J. Bloino, G. Zheng, J. L. Sonnenberg, M. Hada, M. Ehara, K. Toyota, R. Fukuda, J. Hasegawa, M. Ishida, T. Nakajima, Y. Honda, O. Kitao, H. Nakai, T. Vreven, J. Montgomery, J. A., J. E. Peralta, F. Ogliaro, M. Bearpark, J. J. Heyd, E. Brothers, K. N. Kudin, V. N. Staroverov, R. Kobayashi, J. Normand, K. Raghavachari, A. Rendell, J. C. Burant, S. S. Iyengar, J. Tomasi, M. Cossi, N. Rega, J. M. Millam, M. Klene, J. E. Knox, J. B. Cross, V. Bakken, C. Adamo, J. Jaramillo, R. Gomperts, R. E. Stratmann, O. Yazyev, A. J. Austin, R. Cammi, C. Pomelli, J. W. Ochterski, R. L. Martin, K. Morokuma, V. G. Zakrzewski, G. A. Voth, P. Salvador, J. J. Dannenberg, S. Dapprich, A. D. Daniels, O. Farkas, J. B. Foresman, J. V. Ortiz, J. Cioslowski and D. J. Fox, *Gaussian 09, Revision A.02*, Gaussian, Inc., Wallingford CT., 2009.
31 Y. Zhao and D. G. Truhlar, *Theor. Chem. Acc.*, 2008, **120**, 215–241.
32 A. D. Becke, *J. Chem. Phys.*, 1996, **104**, 1040–1046.
33 C. Lee, W. Yang and R. G. Parr, *Phys. Rev. B*, 1988, **37**, 785–789.
34 A. Gutiérrez-Quintanilla, M. Chevalier, J. Ceponkus, R. R. Lozada-García, J. M. Mestdagh and C. Crépin, *Faraday Discuss.*, 2018, **212**, 499–515.
35 C. J. Seliskar and R. E. Hoffmann, *J. Mol. Spectrosc.*, 1982, **155**, 146–155.
36 C. J. Seliskar and R. E. Hoffmann, *J. Mol. Spectrosc.*, 1981, **88**, 30–40.
37 P. R. Bunker, *Molecular Symmetry and Spectroscopy*, Academic Press Inc, New York San Francisco London, 1979.
38 F. Gatti, B. Lasorne, H.-D. Meyer and A. Nauts, *Applications of Quantum Dynamics in Chemistry*, Springer International Publishing, Springer., 2017.
39 Z. Bacic, D. Benoit, M. Biczysko, J. Bowman, S. Bradforth, T. Burd, G. Chambaud, D. Clary, C. Crépin, M. Dracinsky, P. Felker, I. Fischer, F. Gianturco, M. Hochlaf, K. Kouril, I. Kratochvilova, C. M. Liu, A. McCoy, J. Miyazaki, H. Mouhib, J. Richardson, P. Slaviček, T. Stoecklin, K. Szalewicz, A. van der Avoird and A. Zehnacker-Rentien, *Faraday Discuss.*, 2018, **212**, 569–601.

Table of contents entry

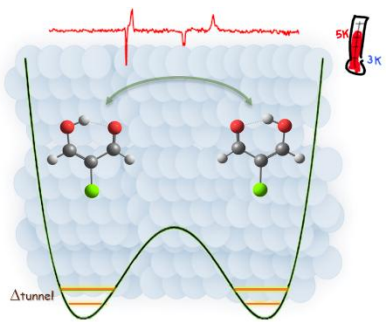

Trapping 2-chloromalonaldehyde in solid *para*-hydrogen is used for a powerful insight on H-tunneling process in various vibrational levels.